Atmos. Chem. Phys., 10, 7457–7466, 2010
www.atmos-chem-phys.net/10/7457/2010/
doi:10.5194/acp-10-7457-2010

Atmospheric Chemistry and Physics

NO_2 photolysis frequencies in street canyons

P. Koepke[1], **M. Garhammer**[1], **M. Hess**[1], **and E.-P. Roeth**[2]

[1]L-M University Munich, Meteorological Institute, Theresienstr. 37, 80333 Munich, Germany
[2]Research Centre Jülich GmbH, ICG1-Stratosphere, Leo Brandt Strasse, 52425 Jülich, Germany

Received: 16 March 2010 – Published in Atmos. Chem. Phys. Discuss.: 18 May 2010
Revised: 21 July 2010 – Accepted: 22 July 2010 – Published: 10 August 2010

Abstract. Photolysis frequencies for NO_2 are modeled for the conditions in urban streets, which are taken into account as canyons with variable height and width. The effect of a street canyon is presented with absolute values and as a ratio *RJ* of the photolysis frequency within the street compared to that with free horizon. This allows further use of the existing photolysis parameterizations. Values are presented for variable solar elevation and azimuth angles, varying atmospheric conditions and different street properties. The NO_2 photolysis frequency in a street depends strongly on the relative width of the street and its orientation towards the sun. Averaged over atmospheric conditions and street orientation, the NO_2 photolysis frequency is reduced in comparison with the values for free horizon: to less than 20% for narrow skyscraper streets, to about 40% for typical urban streets, and only to about 80% for garden streets. A parameterization with the global solar irradiance is given for the averaged *RJ* values.

1 Introduction

Nitrogen dioxide (NO_2) is a key component in the chemistry of the atmosphere. It links the reaction cycles of hydrogen and the halogen species by forming metastable constituents like HO_2NO_2 or $ClONO_2$. In the troposphere, NO_2 controls the concentrations of the peroxy radicals and, hence, the photochemical production of ozone.

In humans, NO_2 causes respiratory diseases and other ailments (Kirsch et al., 2002). As a toxic component of the air, NO_2 is subject to regulations and it is monitored regularly. Licensing procedures (e.g. TA-Luft, 2002), as well as the prediction of the NO_2 and the ozone burden (Elbern et al., 2007), depend on model calculations of atmospheric photochemistry. For such modeling purposes, the exact knowledge of the actual NO_2 photolysis frequency is essential.

Correspondence to: P. Koepke
(peter.koepke@lmu.de)

The photolysis frequency of a chemical substance is given by the equation

$$J = \int F(\lambda)\, \sigma(\lambda, T)\, \Phi(\lambda, T)\, d\lambda \qquad (1)$$

where $F(\lambda)$ is the spectral actinic solar flux, $\sigma\ (\lambda, T)$ the wavelength and temperature dependent absorption cross-section of the substance, and $\Phi\ (\lambda, T)$ the quantum yield of the specific reaction.

The actinic flux is determined as

$$F(\lambda) = \int_0^{2\pi} \int_{-1}^{+1} I\,(\lambda; \vartheta, \varphi)\, d(\cos\vartheta)\, d\varphi \qquad (2)$$

with $I\,(\lambda; \vartheta, \varphi)$ being the spectral radiances of the sky, of the direct sun, and of the radiation reflected at the surface, from any direction of both hemispheres, defined by the zenith angle ϑ and the azimuth φ.

For a given chemical reaction, the NO_2 absorption cross-section and the quantum yield at a given wavelength are available from laboratory measurements (Keller-Rudek and Moortgat, 2010). They depend only slightly on temperature. The actinic flux, however, is highly variable since it is a function of the actual radiation conditions, the spectral field of direct, diffuse and reflected radiation. Thus the actinic flux depends on the solar zenith angle and on the scattering and absorption processes in the atmosphere, i.e. on the amount and type of the aerosol particles, the absorbing gases, the air molecules and the surface albedo. For the photolysis frequency of NO_2 the radiation in the range below 420 nm is of interest, with a relatively large amount of diffuse radiation. Since the radiances from all directions participate in the actinic flux with equal importance, also the radiances from directions with large zenith angle contribute essentially.

In a street canyon, the radiances from the sky and the sun at large zenith angles may be obstructed by the buildings. For these conditions the radiation that is reflected at the walls of the buildings contributes to the actinic flux instead of the radiances from the masked parts of the sky or the sun. These radiances, in general, are much lower than the obstructed radiation, since the albedo of the materials of the buildings is low in the spectral range of interest. Thus, the actinic flux in a street canyon, and consequently the NO_2 photolysis frequency, is strongly reduced compared to that for the same atmospheric conditions, but with a free horizon. Since the street canyon effect is a systematic one, the effect should be taken into account, if the NO_2 photolysis frequency is to be determined for urban conditions.

The NO_2 photolysis frequencies for the conditions in a street are modeled considering variable values of the solar zenith angle and of the sun's azimuth relative to the street. The influence of the relative width of the street canyon, of the aerosol amount and absorption, of the ozone column density, and of clouds is analyzed additionally.

In general, for simplification with respect to the short computational time that is available in photochemical models, the photolysis frequencies are given with simple parameterizations (Roeth, 2002; Trebs et al., 2009). Thus, in the present paper, ratios of the photolysis frequency in the street and its value for the same atmospheric conditions, but with free horizon, are derived. Using these ratios, the application of the existing parameterizations can easily be expanded to the photolysis rates in street canyons.

2 Model and data

2.1 Radiative transfer model

The photolysis frequencies in this study are modeled via spectral radiances, which are determined with the actual version of the System for Transfer of Atmospheric Radiation (STAR) (Koepke et al., 2006; Ruggaber at al., 1994). STAR is a one-dimensional radiative transfer model that determines photolysis frequencies for very different chemical reactions in a fast version (Ruggaber et al., 1994). Besides this, the spectral irradiances, actinic fluxes and radiances are simulated. The radiances depend on the solar elevation, the state of the atmosphere and the ground properties. The atmosphere is described by height-resolved fields of the radiative properties of air molecules, aerosols, ozone, and clouds. The high quality of the model was demonstrated in comparisons with measured and modeled data (Koepke et al., 1998; De-Backer et al, 2001).

To model the variation of the radiation field as an effect of a street canyon, the Sky Obstruction Program SKOP (Hess and Koepke, 2008) is used. The modelling procedure is started with a STAR model run for the solar and atmospheric conditions in question. This model run yields a complete hemispheric spectrally resolved radiance field. Next, the properties of the objects, which are obstructing parts of the sky, are given with their size, shape, and position in terms of their angular dimensions in zenith and azimuth, as seen from the position of the volume for which the actinic flux is calculated. These objects are defined by an arbitrary number of zenith-azimuth angle combinations relative to the sun, under the assumption that the objects are flat. For buildings, the transparency, which could also be taken into account in the program, is zero. Thus the radiances from the sky behind the buildings are omitted and instead the radiation from sun and sky that is reflected at the buildings is taken into account. The spectral irradiances impinging on the walls are calculated by a computer code to get irradiances on arbitrarily oriented receivers (Mech and Koepke, 2004), using the first, undisturbed radiation field. The surfaces are assumed to have Lambertian reflectance with a given albedo, resulting in spectral radiances coming from the walls, which are added to the original radiance field by replacing those sky radiances that are obstructed by the objects. Finally the radiances are integrated to form the spectral actinic flux. Always the total (4π sr) actinic flux is simulated.

It has to be noted that no interaction between the different objects are considered in the model. That means, there are no shadows from one object falling on the other, and there is also no reflection between such objects. These effects are considered to be of minor importance because of the usually low reflectance of the building material in the short wavelength regime. For the purposes described in this paper, the complete hemispherical radiance fields have been calculated with a 1° resolution in zenith and azimuth angle and a spectral resolution of 10 nm.

To get the NO_2 photolysis frequencies, the spectral actinic flux values are multiplied with the relevant absorption cross-sections and quantum yields and spectrally integrated. The atmospheric conditions, the solar position and the characteristics and orientation of the street canyon influence the spectral values of the actinic flux, but not the absorption cross-sections and the quantum yields. However, the processes are strongly wavelength dependent, due to the variable spectral distributions of the radiances over the sky for different atmospheric conditions and solar elevation. Thus, the final effects of the street canyons have to be discussed on the basis of the NO_2 photolysis frequencies

In addition to the photolysis frequencies within various streets, the values for a free horizon have been calculated, using the same atmospheric conditions. The results have been used to determine the ratios between street and free conditions. Such ratios depend only on the variable spectral actinic fluxes, i.e. the properties of atmosphere and of ground, and not on the chemical reactions of the photolytic processes. Thus, these ratios offer the possibility to convert photolysis frequencies from available parameterizations, which in general are valid for undisturbed conditions, into photolysis frequencies for a street canyon.

2.2 Atmospheric properties

The solar irradiation of the earth is described with spectral data for the extraterrestrial sun (Woods et al., 1996), and a relative sun-earth distance which is fixed to 1 as average condition. The solar zenith angle (SZA) is varied between 1° and 85°. The photolysis is modelled under the assumption of an altitude of 200 m above sea-level. The regional albedo, which is used to model the undisturbed irradiance, is set to 3%. This value has been chosen since the albedo in the short wavelength range is generally low (Feister and Grewe, 1995). Additionally, it is decreased due to the urban irregularities (Aida, 1982). The scattering air molecules are considered to be at a barometric pressure of 980 hPa, appropriate to the altitude. The total amount of ozone in the column is mostly fixed to 320 DU. However, also 260 and 400 DU have been tested to demonstrate that an effect due to ozone variation is negligible for NO_2 photolysis frequencies, which is a consequence of its spectral weighting (see Fig. 3).

The aerosol properties are varied between clear, average and turbid conditions. Not only the aerosol amount is changed with the turbidity, but also the aerosol type, which is a mixture of different components, and thus of its absorption properties (Hess et al., 1996). For clear conditions, the aerosol optical depth (AOD) at 550 nm is set to 0.05 and for the aerosol in the boundary layer the type "clear continental" is used. For more polluted conditions, both the AOD and the type is changed: for average conditions the AOD at 550 nm is 0.2 and the type "continental average" and for turbid conditions the AOD is set to 0.4 and the type to "continental polluted" (Hess et al., 1996). Depending on the aerosol type, the spectral values of all optical aerosol properties vary, not only the extinction coefficient, but also the single scattering albedo and the phase function. Since the aerosol particles influence the distribution of the sun and sky radiances, and, as a consequence, the effects of the street buildings, the aerosol absorption and aerosol optical depth have been tested independently. The aerosol amount and its properties are changed in the boundary layer, given as a layer with constant mixture up to 1 km above ground. For the free troposphere, background aerosol is used.

The effect of clouds is modeled for a stratus cloud layer with a vertical extension of 1 km. The clouds obstruct the radiation of the direct sun completely. Thus, an influence of shadow of the buildings, which is partly responsible for the street effect, is negligible for these conditions.

For the calculation of the photolysis frequency according to Eq. (1) the NO_2 spectrum by Mérienne et al. (1995) is applied. The quantum yield is expressed by a Fermi-function

$$\Phi(\lambda) = \frac{1}{1+\exp(0.35(\lambda-\lambda_0)/\mathrm{nm})} \tag{3}$$

which represents the data published by Troe (2000) within the error bars.

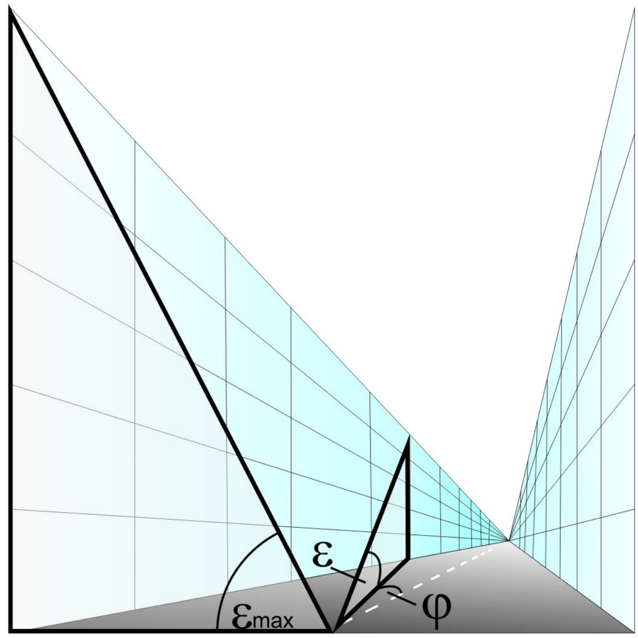

Fig. 1. Angles used to describe the illumination in a street canyon.

The values are slightly temperature-dependent, but the temperature is fixed to 298 K in the calculations. Therefore, neither for the absorption spectrum nor for the quantum yield a temperature effect is considered. Compared to the other variables, the temperature variation is only a second order effect. Moreover, as the paper is focused on the ratios of the photolysis frequencies within the streets and those under undisturbed conditions, but at the same temperature, any temperature effect is further reduced.

2.3 Description of the street canyons

The street under consideration is assumed to have a total width b and the bordering buildings the height h. The actinic flux, and hence the photolysis frequencies, are modeled for a position close to the surface in the middle of a street (Fig. 1). Consequently, the elevation angle of the buildings perpendicular to the street, i.e. the condition for maximum elevation, ε_{max} is given by

$$\tan(\varepsilon_{max})=2h/b \tag{4}$$

The street is assumed to be endless. Thus, the equation for the elevation of the buildings for any direction shifts to

$$\tan(\varepsilon)=2h\sin\varphi/b \tag{5}$$

with φ the azimuth angle against the orientation of the street ($\varphi=90°$ for the direction perpendicular to the street orientation).

The reduction of the actinic flux due to the shadow in the street, and therefore the reduction of the photolysis frequency, depends, of course, on the width of the street canyon

Fig. 2. A typical urban street (Munich): The height of the buildings equals the width of the street.

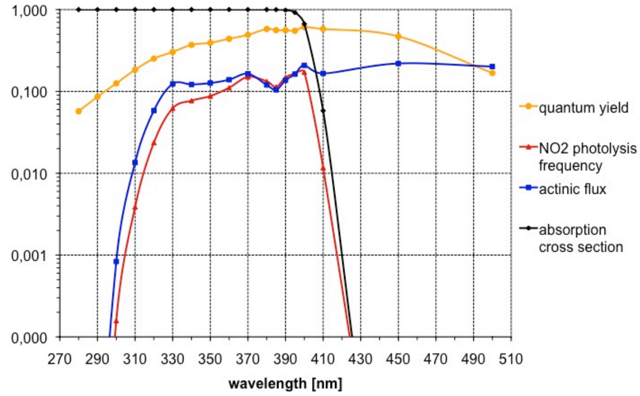

Fig. 3. Spectral values of NO_2 photolysis frequency and of its contributors in relative values.

relative to the height of the buildings. To take this variability into account, the street effects are determined for three different street types: urban street, skyscraper street and garden street.

Urban streets in general have a total width that is in same order of magnitude as the height of the buildings, e.g. with values of about 18 m as shown in Fig. 2 for a typical street in Munich. From $h = b$, for the urban street, the angular elevation of the buildings as function of the azimuth φ is given by

$$\varepsilon = \arctan(2\sin\varphi), \text{ with } \varepsilon_{max} = 63° \quad (6)$$

For a street in an area with skyscrapers $h = 4\ b$ is assumed as ratio, resulting in $\varepsilon_{max} = 83°$.

In a typical suburban street the houses are lower and standing in gardens, resulting in a larger width of the street. These conditions are expressed as $h = b/4$, resulting in $\varepsilon_{max} = 27°$.

The albedo of the street surface and of the walls of the buildings is set to a mean value of 8%, independent of the wavelength. Different material types show some variation of the albedo, but the values are always low in the spectral range of interest (Feister and Grewe, 1995; Bucars, 2006). Moreover, the structure of the walls often produces a certain amount of shady areas, which reduce the average reflection of the buildings.

3 Results

3.1 NO_2 photolysis frequencies

Figure 3 shows the wavelength dependence of the quantities entering the NO_2 photolysis frequency J_{NO_2} on a logarithmic scale. To concentrate on one axis in the figure, the values of all quantities are multiplied by an individual factor which brings the maximum into the range between 0.1 and 1. The NO_2 photolysis frequency has its maximum between 360 and 410 nm, resulting from the actinic flux, which increases with wavelength, and the quantum yield, which is strongly decreasing around 420 nm. Additionally shown is the absorption cross section (yellow), which however, does not vary very strongly with wavelength.

Spectrally integrated values of the NO_2 photolysis frequencies J_{NO_2} (in 1/s) are the final result of the sensitivity study. Such values are depicted in the following figures as a function of the solar zenith angle (SZA). The modeled data are given by the symbols, the connecting lines in between are given only as a guidance for the eye. In general, values are presented for conditions with a free horizon and for a position at the bottom of the street canyon. These values are shown both for the sun shining parallel ($\varphi = 0°$) and perpendicular to the street ($\varphi = 90°$), with the sun's azimuth modeled independently of the solar zenith angle.

Figure 4 shows the NO_2 photolysis frequency J_{NO_2} for average, cloud-free atmospheric conditions both for free horizon and for the three types of street canyons which are taken into consideration, each with the sun shining parallel and perpendicular to the street.

The values J_{NO_2} for undisturbed conditions become smaller with increasing SZA, due to the reduced actinic flux for lower solar elevation. The photolysis frequency in the street canyons also decreases with increasing SZA, but $J_{NO_2}^{street}$ is always additionally reduced, since a part of the sky is obstructed by the buildings. Thus the reduction of the J_{NO_2} increases with the deepness of the street canyons, from garden to skyscraper streets. In the case of shadow, which is given for a SZA where the solar elevation is too low to illuminate the bottom of the street, the direct sun no longer contributes to the actinic flux. Thus, for the conditions with the sun shining perpendicular to the street, a strong decrease of the photolysis frequencies occurs between 5° and 10° SZA for the skyscraper street, between 25° and 30° for the urban street, and between 60° and 65° for the garden street.

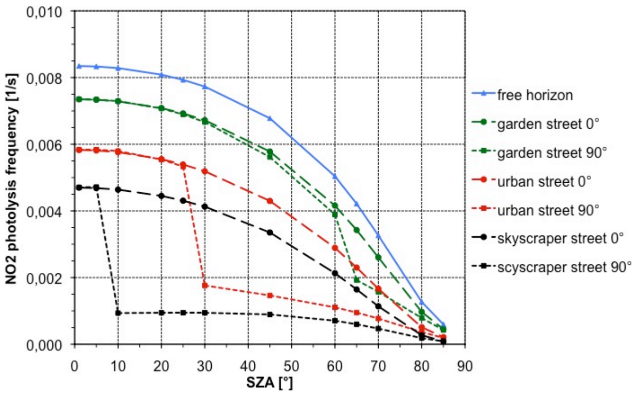

Fig. 4. J_{NO_2} as function of the solar zenith angle for a cloud-free atmosphere with average turbidity for undisturbed conditions with free horizon and for three street types with street orientation parallel ($\varphi = 0°$) and perpendicular to the sun ($\varphi = 90°$).

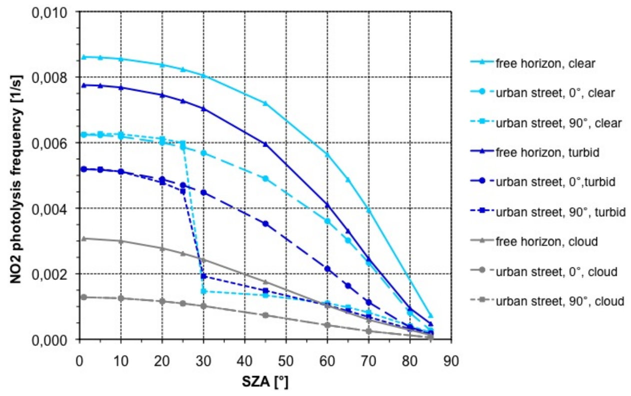

Fig. 5. J_{NO_2} as function of the solar zenith angle for a cloud-free atmosphere with low and with high turbidity and for a cloud obscuring the sun for undisturbed conditions with free horizon and for an urban street with orientation parallel ($\varphi = 0°$) and perpendicular to the sun ($\varphi = 90°$).

For small SZA the sun always illuminates the whole street canyon, with the consequence that the differences between the two azimuth directions are very low. Here $J_{NO_2}^{street}$ can be even slightly larger for the sun shining perpendicular to the street, resulting from the radiation reflected at the houses which are more strongly illuminated under these conditions.

The spectral radiances of sun and sky, and their distribution over the hemisphere depend on the properties of the atmospheric parameters. Thus, also the spectral actinic fluxes and the photolysis frequencies depend on these parameters, and, moreover, their variation due to a street canyon likewise. Figure 5 shows J_{NO_2} and $J_{NO_2}^{street}$ as a function of the solar zenith angle for clean and for turbid, cloud-free atmospheres and for an atmosphere with average turbidity and an additional cloud layer of 1 km thickness. For the conditions with a free horizon, i.e. conditions above the street canyon, the reduction of J_{NO_2} with increasing SZA is to be seen and additionally its reduction with increasing aerosol turbidity. The decrease of the actinic flux due to the assumed cloud layer causes a reduction of J_{NO_2} to about one third of the value for clean, cloud-free conditions. Both, the turbidity and the cloud effects become larger with increasing SZA, as a consequence of the increasing path-length of the radiation through the atmosphere.

The related $J_{NO_2}^{street}$ in Fig. 5 are shown for an urban street canyon with parallel and with perpendicular illumination. As in Fig. 4, the effect of shadow is evident for cloud-free conditions. The reduction for shadow conditions is less pronounced for high turbidity than for low turbidity, due to the sky radiation that increases with turbidity. For the conditions with the cloud layer both azimuth directions of the street result in the same values, since only diffuse radiation exists and thus no shadow due to the buildings occurs.

3.2 Street canyon ratios of NO_2 photolysis frequencies

For an uncomplicated use of photolysis frequencies in chemical models often parameterizations are applied (Röth, 2002). Generally, this is a good approximation when detailed actual conditions are not known. These parameterized photolysis frequencies are normally valid for undisturbed conditions with free horizon, since they are based on values of the global solar irradiance G which are measured for such conditions: $J_{NO_2}^{freehorizon} = f(G)$ (Trebs et al., 2009).

With the help of the ratio RJ of the photolysis frequency in the street canyon $J_{NO_2}^{street}$ and the corresponding values for undisturbed conditions $J_{NO_2}^{freehorizon}$

$$RJ(\text{street properties}, \text{SZA}, \varphi, \text{turbidity}) = \frac{J_{NO_2}^{street}(\text{street properties}, \text{SZA}, \varphi, \text{turbidity})}{J_{NO_2}^{freehorizon}(\text{SZA}, \text{turbidity})} \quad (7)$$

it is possible to determine $J_{NO_2}^{street}$ for conditions where the frequencies for undisturbed conditions $J_{NO_2}^{freehorizon}$ are known. Since the effect is a systematic one, it is possible to use furthermore the existing parameterizations for undisturbed conditions.

$$J_{NO_2}^{street} = RJ\, J_{NO_2}^{freehorizon} \quad (8)$$

Of course, these ratios RJ depend on the properties of the street, on the atmospheric conditions and on the sun's position relative to the street. Thus, in the following figures their variability is displayed, namely the values that finally are used to determine averaged RJ values. Moreover, the variability gives the opportunity to discuss the range of uncertainty for such a general consideration of street canyon effects in the NO_2 photolysis frequencies.

In Fig. 6 the ratios RJ are depicted as a function of the SZA for the same conditions as in Fig. 4, i.e. illuminated street

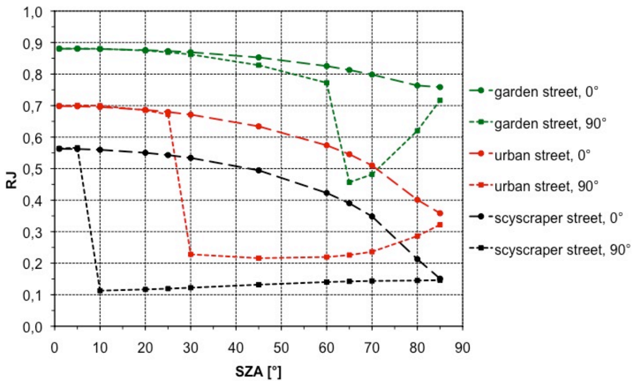

Fig. 6. Ratio *RJ* of NO_2 photolysis frequency in a street canyon and for undisturbed conditions as function of the solar zenith angle for a cloud-free atmosphere with average turbidity for three street types with street orientation parallel ($\varphi = 0°$) and perpendicular to the sun ($\varphi = 90°$).

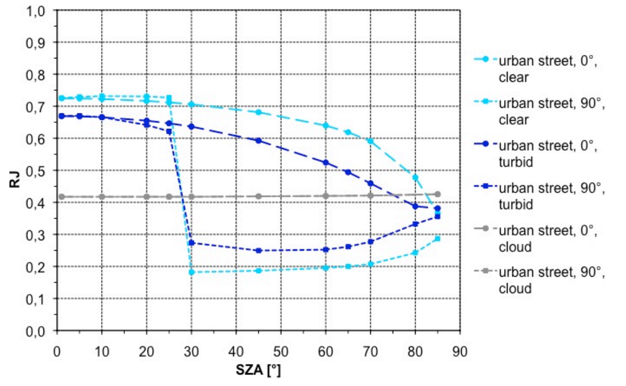

Fig. 7. Ratio *RJ* of NO_2 photolysis frequency in a street canyon and for undisturbed conditions as function of solar zenith angle. for a cloud-free atmosphere with low and with high turbidity and for a cloud obscuring the sun for an urban street with orientation parallel ($\varphi = 0°$) and perpendicular to the sun ($\varphi = 90°$).

canyons of different type under average atmospheric conditions. In each case the sun shines parallel and perpendicular to the street. As mentioned regarding Fig. 4, for zenith angles which are so small that the sun is shining into the street in both cases, the ratios for the two directions are equal. These conditions shift to larger SZA with increasing width of the street compared to the height of the houses.

The reduction of *RJ* with reduced width of the street canyon is evident, since larger parts of the radiation of sun and sky are omitted. For typical urban streets, the ratio is between 0.7 and 0.4 for sunny conditions and between 0.2 and 0.3 in the case of shadow. For the skyscraper streets the radiation reduction due to the buildings is stronger, with *RJ* between 0.55 and 0.2 in the sun and about 0.15 in the shade. Reversely, for wide garden streets the reduction is only small, with *RJ* about 0.85 for sunny and between 0.5 and 0.7 for shady conditions. Fig. 6 again shows that shadow in the street occurs for a wide range of SZA for small streets, but is shifted to conditions with increased SZA for increasing widths of the streets. For sunny conditions, a slight decrease of *RJ* with increasing SZA can be seen for all street types. This results from the fact that the diffuse radiation increases relative to that of the direct sun. Thus, the obstruction of the diffuse radiation becomes more important at larger SZA. For conditions with shadow in the street, *RJ* is slightly increasing with SZA, since for undisturbed conditions the total actinic flux decreases more strongly than the diffuse radiation only. For very large SZA the contribution of the direct sun is very low. This has the effect that the sky's radiation dominates totally, and thus the *RJ* values become similar for both, the sun shining parallel and perpendicular to the street.

The photolysis frequency ratio for different atmospheric conditions is shown in Fig. 7 as a function of SZA for an urban street, analog to Fig. 5. For cloud-free conditions, the effects of sun and shadow become obvious again. As mentioned, the aerosol absorption is assumed to increase with increasing AOD, resulting in larger absorption for high than for low turbidity. In the actinic flux for free horizon, for small SZA the effect of absorption is dominant while for large SZA the extinction and thus the aerosol optical depth is of higher relevance. The trend of *RJ* with SZA can be explained by combination of the different contributions of sun and sky to $J_{NO_2}^{freehorizon}$ and to $J_{NO_2}^{street}$. In case of shadow, the diffuse radiation dominates, and, hence, *RJ* increases with turbidity, and for sunny conditions the reverse is true. In comparison to the conditions with average turbidity (Fig. 6) it can be seen that the variation of the aerosol properties produces an uncertainty of *RJ* in the order of ±0.05.

Clouds in front of the sun reduce the actinic flux in general. If the cloud has such a large optical thickness that the direct sun is no longer of relevance, as modeled, the values are the same for the two azimuths between sun and street and nearly independent of SZA. The data are results for overcast conditions, but the effect of missing building shadows would be similar also for a single thick cloud in front of the sun. As shown in Fig. 7, *RJ* for the condition with a cloud obscuring the sun is between that for sunny and for shady scenarios, since the buildings do not cast a shadow. *RJ* is about 0.4 for conditions without direct sun for a typical urban street canyon. A slight increase of *RJ* with SZA results from the fact that the total irradiance is more strongly reduced due to solar elevation than the radiation from the zenith region.

The photolysis frequencies under cloudy conditions and the corresponding *RJ* are not shown for the other street types as they are nearly constant for the different SZA and street azimuths. The values are about 0.8 for garden streets and about 0.17 for the skyscraper streets.

The effects of the aerosol amount and absorption, as independent variables, and of the ozone column density are analyzed, but not displayed. Their effect on $J_{NO_2}^{street}$ is negligible in comparison to the other effects. The *RJ* are determined for fixed average AOD, but variable aerosol absorption, on the one hand, and with fixed average absorption but variable AOD, on the other hand. The effect on *RJ* differs a bit for the conditions in the sun and those with shadow, but in every case the variation in *RJ* is much less than that between a clean and a turbid atmosphere. Variations in total atmospheric ozone influence the UV actinic flux, but this effect can be neglected in the spectral range relevant for the NO_2 photolysis frequencies (See Fig. 3). Thus, the values *RJ* do not depend on the total ozone. Of course, this effect has to be separated from the chemical reactions in the street which form NO_2, and which depend directly on the local ozone concentration.

4 Parameterization with the global irradiance

Parameterized photolysis frequencies (Röth, 2002) are available only for undisturbed conditions with free horizon, since they are based on values of the global solar irradiance G, measured for such conditions (Trebs et al., 2009).

Using adequate ratios *RJ*, the $J_{NO_2}^{street}$ frequencies for a street canyon can be determined from the values for undisturbed conditions $J_{NO_2}^{freehorizon}$ derived with the existing parameterization schemes. To achieve an easy availability of the corresponding *RJ*, they should also be parameterized versus the global solar irradiance G which already is used to get $J_{NO_2}^{freehorizon}$. Such a correlation, of course, can take into account only the variability of the atmospheric and solar conditions. The individual width and orientation of a street canyon has to be considered independently.

In general, neither the atmospheric conditions nor the street properties are known. Thus, average *RJ* are determined which are valid for average conditions, and connected with the global solar irradiance. The average ratios *RJ* are derived from the values for the three different conditions that have to be taken into account. These are atmospheric conditions with no cloud obscuring the sun, i.e. with free sun, either with the street in the sun, RJ_{sun}, or in the shadow, RJ_{shad} , and conditions where the sun is obscured by a cloud, RJ_{cloud}. These data are available for the different street types, as discussed above.

To get an average value of *RJ*, the *RJ* for the three possible conditions mentioned above have to be weighted with their relative contribution. This is done by factors called F_{sun}, F_{shad} , and F_{cloud} , which depend on the atmospheric conditions and the street azimuth, resulting in a final *RJ* by

$$RJ = F_{sun} RJ_{sun} + F_{shad} RJ_{shad} + F_{cloud} RJ_{cloud} \tag{9}$$

Of course, the weighting factors sum up to 100%.

$$F_{sun} + F_{shad} + F_{cloud} = 1 \tag{10}$$

Since G will be used for the parameterization, but the *RJ* are available for SZA, in a first step G is correlated to SZA for average conditions. Figure 8 shows G as a function of SZA for cloud-free conditions under average turbidity (see Schulze, 1976; Iqbal, 1983). For situations with clouds obscuring the sun, G is assumed to be reduced to 40% compared to cloud-free conditions on the average. To get the SZA which are needed for the correlation of *RJ* and G, G is investigated in steps of 50 W/m^2.

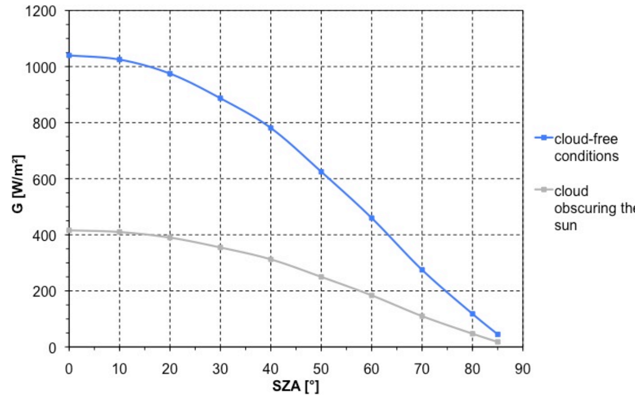

Fig. 8. Global solar irradiance as function of solar zenith angle for average cloud-free conditions and for conditions with a cloud obscuring the sun.

Global irradiance with $G > 450$ W/m^2 is assumed to occur only for conditions with no cloud obscuring the sun. Thus, for these conditions always F_{cloud} equals 0 and only conditions with the street in the sun or in the shadow of the buildings have to be separated, resulting in $F_{sun} + F_{shad} = 1$. The sun shines into the street if SZA is less than $(90° - \varepsilon)$. This condition is used to get the appropiate values of the azimuth φ_{sun} according to Eq. (5). For all $\varphi < \varphi_{sun}$ the street is illuminated by the sun. Since normally the orientation of the street is not known, the assumption is made that it is random. Thus, the probability for the street in the sun is given by φ_{sun} divided by the total possibility of relevant orientation of 90°, resulting in

$$F_{sun} = \varphi_{sun}/90 \tag{11}$$

and, as a consequence,

$$F_{shad} = 1 - F_{sun} \tag{12}$$

Of course φ_{sun} depends on the SZA, which for the parameterization is correlated to G. For high sun, i.e. small values of SZA, the sun may shine always into the street, resulting in $F_{sun} = 1$, and for low sun the conditions with a sunny street are reduced to a small range of φ_{sun} values close to 0°, resulting in low values of F_{sun}. Since φ_{sun} also depends on ε, F_{sun} and F_{shad} are determined individually for the three different street types considered.

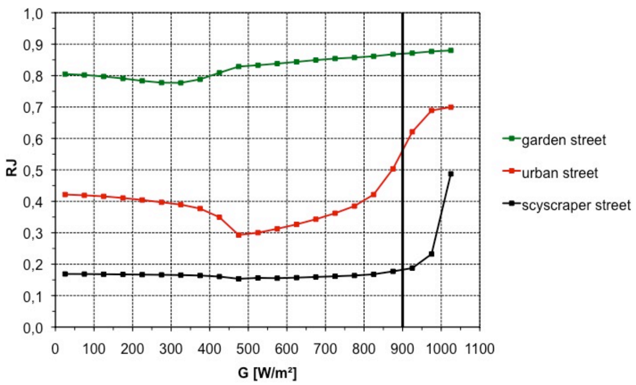

Fig. 9. Ratio *RJ* of NO_2 photolysis frequency in a street canyon and for undisturbed conditions as function of the solar global irradiance *G* for three street types. The values are averaged over the street orientation and the meteorological conditions (see text). The vertical line at 900 W/m^2 cuts out conditions with global solar irradiance that, in general, do not occur for mid latitudes.

For conditions with $G<450$ W/m^2 it cannot be decided without additional information whether the irradiance is valid for cloud-free conditions with large SZA or for those with a smaller SZA, but a cloud obscuring the sun. Since the desired parameterization uses only *G* as information, an assumption is made with respect to the probability that clouds obscure the direct sun. With respect to the fact that in a layer with broken cloudiness from the sun's perspective the gaps between the clouds become smaller with increasing SZA, F_{cloud} is varied between 0.5 for vertical sun and 1 for the sun at the horizon, taking into account the increasing length of the path through the atmosphere with increasing SZA.

Averaged *RJ* as a function of *G* are determined for the three street types by Eq. (9), using the derived *F*-values as a function of SZA and the related RJ_{sun} , RJ_{shad} and RJ_{cloud} for atmospheric conditions with average turbidity, as shown in Fig. 6. These averaged *RJ* are presented in Fig. 9 as a function of the solar global irradiance. The *RJ* values are large, i.e. the reduction of the photolysis frequency is low, for the garden street. *RJ* becomes lower for the urban and for the sky scraper street, caused by the increasing reduction of sky radiation and the increased probability of shadow in the street. For all street types *RJ* has high values for large values of *G*, since the large values of global irradiance only occur for cloud-free conditions at small SZA. The probability for such conditions is shifted to lower values of *G* with increasing street width. For decreasing values of *G*, but cloud-free conditions, the averaged *RJ* are reduced due to the increasing probability of shadow. For values of *G* less than 450 W/m^2, where clouds are assumed to be of relevance, the *RJ* values increase a bit for the smaller streets, since the relative contribution of the visible part of the sky increases for cloudy conditions. For the wide garden street the influence of shadow is low, with the consequence that the possibility of a cloud reduces *RJ*. With decreasing *G* the probability of clouds obstructing the sun increases, with the effect that for $G<100$ W/m^2 the averaged *RJ* equal the values for cloudy conditions. The *RJ* for clouds obscuring the sun is nearly independent of SZA and therefore independent of *G*. As a consequence, the relative minimum in the averaged *RJ* in Fig. 9 results from conditions with increased probability for shadow in the street, but without clouds.

For the conditions at mid-latitudes, like in Europe, only solar zenith angles larger than 25° are of relevance. Since this results commonly in $G<900$ W/m^2, the large values of averaged *RJ*, as shown in the right part of Fig. 9, are of no relevance for mid-latitudes.

5 Uncertainty of *RJ*

The *RJ* value depends strongly on the individual relation of the width of the street to the height of the buildings. Therefore, these effects are varied in a realistic range, considering three street types, from which the user may select the appropriate *RJ*.

In general, the azimuth orientation of individual streets cannot be incorporated into chemical models and thus the effect is accounted for in the averaged *RJ*, depicted in Fig. 9 as a function of the solar global irradiance *G*. The *RJ* averaged over street orientation and meteorological conditions, as modeled by Eq. (9), depend on the reflection properties of the street and the buildings, and on the atmospheric conditions. The optical thickness of the clouds has only a negligible effect, since cloud shadow can be assumed whenever the cloud is thick enough to block out the direct sunlight. The effect of the uncertainty of the aerosol type and amount, shown in Fig. 7, is in the order of $\pm$ 0.05. For the averaged *RJ* this uncertainty range is even reduced, since increasing aerosol optical depth has a converse effect on the direct sun and on the sky irradiance, which thus partly cancel out each other. The effect of the somewhat uncertain reflection properties of the surface and the buildings is also not large, since in any case the buildings obscure the sky radiation from behind. The same holds true for the multiple reflections between the buildings, which are not taken into account here.

The correlation of *RJ* with the global irradiance *G* results in a further uncertainty due to the assumptions on the cloudiness with respect to SZA and *G*. Thus, the uncertainty of *RJ* belonging to a street type and a known *G* is estimated to be in the order of $\pm$ 0.1.

For an individual street, the *RJ* values are even more uncertain due to the street azimuth relative to the sun. With respect to this, the possible variability of *RJ* lies between the values for sun and for shadow, as shown in Fig. 6. This effect must be accounted for if conditions for a specific street are of interest, for example to verify measured data. Moreover, it has to be considered that the relevant azimuth is changing during the day, as a consequence of the course of the sun.

Table 1. Averaged reduction factors *RJ* for different street types.

street type	building height/street width	range of *RJ* for $G<900\,W/m^2$	average *RJ*
free horizon	0	1	1
garden street	0.25	0.75–0.9	0.8
urban street	1	0.3–0.5	0.4
skyscraper street	4	0.15–0.2	0.17

And finally, it must be said that for the complex NO_X reaction system the photolysis frequencies are only one aspect besides the varying concentrations of the trace gases. So, in an actual case, it should be considered that the chemical substances in the windward and the leeward side may be different. The same holds true for the *RJ* on the sidewalks where the measurements usually take place, since the data shown in this paper are valid for conditions in the middle of the canyon near the street surface.

6 Conclusion and discussion

Street canyons reduce the NO_2 photolysis frequency compared to that for undisturbed conditions with free horizon. This reduction is low for sunny conditions, and quite large for a volume in the shadow of buildings. In the case of an overcast sky, or with a cloud obstructing the sun, the shadow of buildings is of no relevance. The canyon effect reduces the photolysis frequency normally to values between that for shadow and sun. The J_{NO_2} reduction is high for narrow streets and high buildings and less pronounced for wider streets and lower houses, due to the relative amount of radiation that is obstructed by the buildings. The variability of the effect under different atmospheric conditions can be reduced, if the ratio *RJ* is considered instead of the absolute NO_2 photolysis frequency. *RJ* is the quotient of the photolysis frequency in the street and that under the same atmospheric conditions, but with a free horizon.

Generally, for an easy handling in chemistry models, a parameterization of the NO_2 photolysis frequency depending on the global solar irradiance G is used. Therefore, such a parameterization is also derived for *RJ*, with averaged values that take into account all aspects of the variability besides the street type.

For regions with solar zenith angles less than 25°, like in Europe, the global solar irradiance G is usually less than $900\,W/m^2$. For these conditions the averaged *RJ* values show only a small variability with respect to G, as depicted in Fig. 9. Therefore, in Table 1 *RJ* values are given for the street types under consideration that are not only means over the meteorological conditions and the street orientation, but additionally averaged over the solar irradiance G.

As shown, the relative width of the street strongly changes the actinic flux in the street and thus the photolysis frequency and the *RJ* values. Here, a more precise statistical analysis of the streets in the area of investigation would be helpful. This involves also the actual reflection properties of the buildings and the relevant atmospheric conditions like cloudiness and turbidity. For values of the global irradiance where cloud effects are possible ($G<450\,W/m^2$), additional knowledge of SZA would allow the decision whether a cloud is obscuring the sun or not. And if the azimuth of a street is known, it could be used to determine individual *RJ* and their change during the day. However, all these aspects are far beyond the idea of this paper, and such additional information is most likely not applicable for routine conditions.

On the contrary, simply one general reduction factor *RJ* could be of interest, independent of street type and orientation, for an easy use of the photolysis frequency in street canyons in chemical models. If only one general *RJ* should be used to modify the NO_2 photolysis frequencies from a free horizon to a street canyon, we suggest $RJ=0.5$. Of course, this value will be uncertain, in the worst case by ± 0.5. But it considers the systematic reduction of the NO_2 photolysis frequencies in street canyons and corresponds to the fact that photolysis frequencies are only one aspect in the complex air chemistry.

Acknowledgements. Financial support by the German Umweltbundesamt under UFOPLAN Grant 370942207 is gratefully acknowledged.

Edited by: I. Trebs

References

Aida, M.: Urban albedo as function of the urban structure, Boundary Layer Meteorology, 23(4), 405–413, 1982

Bogumil, K., Orphal, J., Homann, T., Voigt, S., Spietz, P., Fleischmann, O. C., Vogel, A., Hartmann, M., Bovensmann, H., Frerick, J., and Burrows, J. P.: Measurement of molecular absorption spectra with the SCIAMACHY pre-flight model: Instrument characterization and reference data for atmospheric remote sensing in the 230–2380 nm region, J. Photochem. Photobiol. A, 157, 167–184, 2003

Bucars, N.: Regionale und lokale Albedo im UV-Spektralbereich, Diploma-thesis, Meteorolog. Inst. Univ. Munich, 46 pp., 2006.

De Backer, H., Koepke, P., Bais, A., de Cabo, X., Frei, T., Gillotay, D., Haite, C., Heikkilä, A., Kaqzantzidis, A., Koskela, T., Kyrö, E., Lapeta, b., Lorente, J., Masson, K., Mayer, B., Plets, H., Redondas, A., Renaud, A., Schauberger, G., Schmalwieser, G., Schwander, H., and Vanicek, K., Comparison of measured and modeled UV indices for the assessment of health risks, Meteorol. Appl., 8, 267–277, 2001.

Elbern, H., Strunk, A., Schmidt, H., and Talagrand, O.: Emission rate and chemical state estimation by 4-dimensional variational inversion, Atmos. Chem. Phys., 7, 3749–3769, doi:10.5194/acp-7-3749-2007, 2007.

Feister, U. and Grewe, R.: Spectral albedo measurements in the UV and visible region over different types of surfaces, Photochem. Photobiol., 62(4), 736–744, 1995.

Hess, M., Koepke, P., and Schult, I.: Optical Properties of Aerosols and Clouds: The Software Package OPAC, B. Am. Meteorol. Soc., 79(5), 831–844, 1998.

Hess, M. and Koepke, P.: Modelling UV irradiances on arbitrarily oriented surfaces: effects of sky obstructions, Atmos. Chem. Phys., 8, 3583–3591, doi:10.5194/acp-8-3583-2008, 2008.

Iqbal, M.: An introduction to solar radiation, Academic Press, Toronto, 1983.

Keller-Rudek, H. and G. M. Moortgat, MPI-Mainz UV-VIS Spectral Atlas of Gaseous Molecules, www.atmosphere.mpg.de/enid/2295, 2010

Kirsch, M., Korth, H.-G., Sustmann, R., and de Groot, H.: The Pathobiochemistry of Nitrogen Dioxide, Biol. Chem., 383, 389–399, 2002

Koepke, P., Bais, A., Balis, D., Buchwitz, M., Backer, H. D., Cabo, X. D., Eckert, P., Erikson, P., Gillotay, D., Heikkilä, A., Koskela, T., Lapeta, B., Littynska, Z., Lorente, J., Mayer, B., Renaud, A., Ruggaber, A., Schauberger, G., Seckmeyer, G., Seifert, P., Schmalwieser, A., Schwander, H., Vanicek, K., and Weber, M.: Comparison of models used for UV Index calculations, Photochem. Photobiol., 67 (6), 657–662, 1998.

Koepke, P., Anwender, D., Mech, M., Oppenrieder, A., Reuder, J., Ruggaber, A., Schreier, M., Schwander, and H., Schween, J.: Actual state of the UV radiation transfer model package STAR, in: IRS2004: Current Problems in Atmospheric Radiation, edited by: Fischer, H. and Sohn, B.-J., A. Deepak Publ., Hampton, USA, 71–74, 2006.

Mech, M. and Koepke, P.: Model for UV irradiance on arbitrarily oriented surfaces, Theor. Appl. Climatol., 77, 151–158, 2004.

Mérienne, M. F., Jenouvrier, A., and Coquart, B.: The NO_2 absorption spectrum: Absorption cross-sections at ambient temperature in the 300–500 nm region, J. Atmos. Chem. 20, 281–297, 1995.

Röth, E.-P.: Description of the Anisotropic Radiation Transfer Model ART to Determine Photodissociation Coefficients, Ber. Forschungszentrum Jülich Jül-3960, ISSN 0944-2952, 2002.

Ruggaber, A., Dlugi, R., and Nakajima, T.: Modelling radiation quantities and photolysis frequencies in the troposphere, J. Atmos. Chem., 18, 171–210, 1994.

Schulze, R.: UV-Strahlenklima, in: Ultraviolette Strahlen, Kiefer, J. (Hrsg.), Walter de Gruyther, Berlin, Germany, 26–27, 1977.

TA-Luft, Technische Anleitung zur Reinhaltung der Luft, Germany, GMBI Heft 25–29, 511–605, 2002.

Trebs, I., Bohn, B., Ammann, C., Rummel, U., Blumthaler, M., Königstedt, R., Meixner, F. X., Fan, S., and Andreae, M. O.: Relationship between the NO2 photolysis frequency and the solar global irradiance, Atmos. Meas. Tech., 2, 725–739, doi:10.5194/amt-2-725-2009, 2009.

Troe, J.: Are Primary Quantum Yields of NO_2 Photolysis at $\lambda \leq 398$ nm Smaller than Unity?, Z. Phys. Chem., 214, 573–581, 2000.

Woods, T. N., Prinz, D. K., Rottman, G. J., London, J., Crane, P. C., Cebula, R.P.,, Hilsenrath, E., Brueckner, G. E., Andrews, M. D., White, O. R., Van Hoosier, M. E., Floyd, L. E., Herring, L. C., Knapp, B. G., Pankratz, C. K., and Reiser, P. A., Validation of the UARS solar ultraviolet irradiances: Comparison with the Atlas 1 and 2 measurements, J. Geophys. Res., 101, 9541–9570, 1996.